Plant Physiol. (1995) 108: 503–516

Hrp Mutant of *Pseudomonas syringae* pv *phaseolicola* Induces Cell Wall Alterations but Not Membrane Damage Leading to the Hypersensitive Reaction in Lettuce[1]

Charles S. Bestwick*, Mark H. Bennett, and John W. Mansfield

Department of Biological Sciences, Wye College, University of London, Ashford, Kent TN25 5AH, United Kingdom

Both wild-type (S21-WT) and *hrpD*⁻ (S21–533) strains of *Pseudomonas syringae* pv *phaseolicola* induced the formation of large paramural papillae in lettuce (*Lactuca sativa*) mesophyll cells adjacent to bacterial colonies. Localized alterations to the plant cell wall included deposition of hydroxyproline-rich glycoproteins, phenolics, and callose, and were associated with proliferation of the endoplasmic reticulum and multivesicular bodies. Tissue collapse during the hypersensitive reaction caused by S21-WT was associated with electrolyte leakage and rapid accumulation of the phytoalexin lettucenin A, both of which followed membrane damage indicated by the failure of mesophyll cells to plasmolyze. A few cells lost the ability to plasmolyze after inoculation with S21–533, and low levels of lettucenin A were recorded, but neither leakage of electrolytes nor tissue collapse were detected. Dysfunction of the plasma membrane in cells adjacent to colonies of S21-WT led to extensive vacuolation of the cytoplasm, organelle disruption, and cytoplasmic collapse—changes unlike those occurring in cells undergoing apoptosis. Strain S21–533 remained viable within symptomless tissue, whereas cells of S21-WT were killed as a consequence of the hypersensitive reaction. Our observations emphasize the subtle coordination of the plant's response occurring at the subcellular level.

The HR has been recognized as an expression of resistance to microbial colonization since the term was used by Stakman (1915) to describe the response of grasses to infection by *Puccinia graminis*. The occurrence of membrane damage, necrosis, and collapse of challenged cells have now been established as common features of the HR, but the early stages of the response remain poorly defined. In particular, the relationship and possible coordination between the induction of membrane damage and activation of other responses such as modification of the cell wall and phytoalexin synthesis are still incompletely understood (Lamb et al., 1989; Mansfield, 1990; Marco et al., 1990; Slusarenko et al., 1991; Mansfield et al., 1994; Mehdy, 1994). The HR occurring in response to fungal infections is often highly localized; for example, the response of lettuce (*Lactuca sativa*) cultivars to the downy mildew fungus *Bremia lactucae* is confined to individual penetrated cells (Woods et al., 1988). In consequence, biochemical analyses of early events during fungal infections are difficult to interpret because responses occurring in comparatively few cells may be masked by a background of unaffected tissue (Mansfield, 1990; Bailey, 1982; Bennett et al., 1994). Because of the spatial and temporal difficulties associated with an examination of the HR induced by fungi, the most detailed knowledge of biochemical and ultrastructural events occurring in cells undergoing the HR has come from work on plant-bacterium interactions in which comparatively large amounts of responding tissue may be obtained (Brown and Mansfield, 1988; Adám et al., 1989; Croft et al., 1990; Marco et al., 1990).

The collapse of plant cells during the HR has been described as an apoptosis, where the challenged cell responds to a particular stimulus by initiating a series of degenerative changes culminating in "suicidal" destruction (Slusarenko et al., 1986, 1991; Dietrich et al., 1994). Preliminary experiments showed that the bacterial halo-blight pathogen of bean, *Pseudomonas syringae* pv *phaseolicola*, caused a rapid and confluent HR after infiltration of suspensions of 10^7 cfu mL^{-1} or more into lettuce leaves (Bestwick and Mansfield, 1992). Challenge by *P.s.* pv *phaseolicola* therefore provided a model system for the analysis of cellular responses occurring during the HR in lettuce.

This article describes studies of the lettuce-*P.s.* pv *phaseolicola* interaction. In addition to experiments with the wild-type, race 6 strain S21-WT, a Tn*5* insertion mutant, S21–533, which has lost pathogenicity and ability to cause the HR in nonhost plants, i.e. has the Hrp⁻ phenotype (Lindgren et al., 1986; Somlyai et al., 1986; Willis et al., 1991), was also examined. Hybridization and complementation experiments show that S21–533 has a single Tn*5* insertion in the *hrpD* locus within the cluster of *hrp* genes identified in *P.s.* pv *phaseolicola* (El-Kady et al., 1986; Nöllenburg et al., 1990; Rahme et al., 1991). The *hrpD* locus has been reported to encode a membrane-associated protein (Miller et al., 1993). Strains S21-WT and S21–533 have

[1] This work was supported by a studentship from the Agricultural and Food Research Council.

* Corresponding author; e-mail c.bestwick@wye.lon.ac.uk; fax 44–12–33–813140.

Abbreviations: cfu, colony-forming unit; HR, hypersensitive reaction; HRGP, Hyp-rich glycoprotein; MVB, multivesicular body; SDW, sterile distilled water; TBST, 20 mM Tris-buffered saline (pH 7.4) containing 0.1% (w/v) BSA and 0.05% (w/v) Tween 20.

already been used for investigations of the consequence of O_2^- generation during the nonhost HR in tobacco. Adám et al. (1989) showed that the failure of the *hrpD* mutant to cause a macroscopic HR was associated with the loss of ability to induce O_2^- generation and extensive lipid peroxidation within infiltrated tissue. The involvement of Hrp proteins in signaling and regulation of the oxidative burst has also been demonstrated by Baker et al. (1993), who found that harpin, the protein product of the *hrpN* gene from *Erwinia amylovora*, stimulates active oxygen production in tobacco and acts as an elicitor of the HR.

In recent studies of the responses of bean leaves to pseudomonads, Jakobek and Lindgren (1993) have shown that *hrp* mutants of *P.s.* pv *tabaci*, although failing to cause a macroscopic HR, did cause the accumulation of mRNA transcripts for enzymes thought to represent defense-related responses, such as Phe ammonia-lyase, chalcone isomerase, chalcone synthase, and chitinase. They also demonstrated accumulation of unnamed phytoalexins detected as zones of inhibition in TLC plate bioassays. Results obtained by Jakobek and Lindgren (1993) contrasted with data from Meier et al. (1993), who found no phytoalexins in bean in the absence of necrosis characteristic of the HR. In lettuce, the development of a sensitive assay for the sesquiterpenoid phytoalexin lettucenin A has allowed the demonstration that accumulation of the antibacterial compound follows irreversible membrane damage (indicated by failure to plasmolyze) in cells undergoing the HR to *B. lactucae* and *P.s.* pv *phaseolicola* (Takasugi et al., 1985; Bennett et al., 1994).

The ability of plant cells to respond in a highly localized manner to the presence of wild-type, phytopathogenic bacteria has been demonstrated by EM of several interactions, for example *P.s.* pv *phaseolicola* and bean (Brown and Mansfield, 1988; Mansfield et al., 1994), *P.s.* pv *pisi* and tobacco (Politis and Goodman, 1978), and *Xanthomonas campestris* pv *vesicatoria* and pepper (Brown et al., 1993). In each case, the response described has been the formation of a cell wall apposition or papilla adjacent to the bacterial colony. In bean and melon, immunogold labeling demonstrated the deposition of HRGPs within papillae (O'Connell et al., 1990). A possible role for HRGPs in agglutinating invading bacteria has been proposed (Leach et al., 1982; Swords and Staehelin, 1993). The significance of the accumulation of HRGPs and other wall-associated proteins in plant defense has recently been reviewed (Bowles, 1990).

Here we describe combined physiological, biochemical, and ultrastructural studies of the responses of lettuce to wild-type and $hrpD^-$ strains of *P.s.* pv *phaseolicola*. We include what to our knowledge is the first report of the reactions of individual plant cells to Hrp^- bacteria; massive but localized cell wall alterations including deposition of HRGPs, phenolics, and callose were detected in the absence of the cell collapse characteristic of the HR. Because the response was observed next to most bacteria, the process of secretion of the deposits could be observed in detail. Analyses of bacterial populations have also shown that Hrp^- strains may survive more successfully than pathogenic bacteria in nonhost plants.

MATERIALS AND METHODS

Growth of Plants

Seeds of *Lactuca sativa* cv Diana were planted in trays containing soil-less compost and germinated under glasshouse conditions at 18 to 24°C. After germination and cotyledon development, seedlings were transplanted to individual pots (10 cm diameter) of compost. Four-week-old plants were removed from the glasshouses and placed in growth-room conditions of 16-h day length (80 W m^{-2} at soil level), 75% RH, and 24°C constant temperature 48 h prior to inoculation. During experiments, plants were maintained under constant illumination.

Bacterial Strains and Plant Inoculation

Isolate S21-WT of *Pseudomonas syringae* pv *phaseolicola* and the *hrp* mutant derived from this strain, S21–533, were kindly supplied by Dr. G. Somlyai of the Hungarian Plant Protection Institute, Budapest (Somlyai et al., 1989).

Strains were loop inoculated into Luria broth supplemented with rifampicin (50 μg mL^{-1}) for S21-WT and rifampicin and kanamycin (25 μg mL^{-1}) for S21–533 in 25-mL Sterilin tubes, and incubated at 25°C on an orbital shaker at 200 rpm for 48 h. Bacteria were pelleted by centrifugation and washed in SDW and their concentration was adjusted to 10^8 cfu mL^{-1} by dilution to give an A_{620} of 0.12 (1 cm light path), as described by Smith and Mansfield (1982). Bacterial suspensions were inoculated by hypodermic syringe (23-gauge needle) into alternate leaf panels of expanded leaves.

Bacterial Multiplication

Bacterial cfus were recovered from inoculated tissues by removing three 1-cm-diameter leaf discs from the region of inoculation. Excised discs were washed briefly in 40% (v/v) ethanol and then rinsed in SDW (2 × 2 min). The discs were homogenized in 200 μL of SDW in 1-mL sterile Eppendorf tubes, and the volume was made up to 1 mL with SDW. Dilutions of the homogenate (1:10, 1:100, 1:500, 1:1000, and 1:2000) were plated onto Kings B agar. Plates were incubated for 48 h at 30°C, and the number of colonies was counted.

Electrolyte Leakage

After inoculation with S21-WT, S21–533, or SDW, five 1-cm-diameter leaf discs were removed from inoculated leaves and washed, with gentle agitation, in SDW to remove electrolytes released from damaged cells. The discs were then blotted dry and placed in 5 mL of SDW in a 10-mL (2-cm-diameter) glass vial. A punctured lid was placed over the leaf discs and the vial was placed in a vacuum desiccator. Discs were vacuum infiltrated for 3 min at 5.0 kPa with the vacuum being broken every 30 s. The bathing solution was then decanted from the leaf discs, filtered through a 0.2-μm filter, and collected in a Sterilin tube, and its conductivity was measured using a Jenway (Essex, UK) 4010 conductivity meter in the range 0 to 200

microsiemens. After measurement, the bathing solution was returned to the leaf discs and the discs were autoclaved at 120°C for 25 min to destroy all cell membranes and placed under vacuum as described, and the total conductivity was measured. Results were expressed as a percentage of the total electrolytes that could be washed from the leaf discs.

Plasmolysis

The ability of cells to plasmolyze during the HR was determined by fixing approximately 4-mm^2 pieces of leaf tissue in 2.5% glutaraldehyde in 50 mM Pipes buffer (pH 7.2) containing a plasmolyzing solution of 0.8 M KNO_3. Tissue was fixed and processed for transmission EM as described below. Sections (0.5 μm) of Epon-Araldite-embedded material were mounted in water on glass microscope slides and air dried. After staining with toluidine blue (0.05% [w/v] in 0.1 M sodium phosphate buffer at pH 7.2) for 30 s at room temperature, excess stain was washed off with SDW and the sections were allowed to dry before examination on a Nikon light microscope.

Phytoalexin Accumulation

The phytoalexin was identified in tissue extracts based on retention time and UV absorption spectrum after HPLC and co-chromatography after "spiking" samples with authentic lettucenin A (Bennett et al., 1994). At each time point, three 1.4-cm-diameter discs of tissue were cut from infiltrated interveinal zones. The tissue was ground in 300 μL of 70% methanol:water in an Eppendorf tube (1.5 mL) with a roughened plastic pestle until a fine suspension was obtained. The sample was then centrifuged at 1600*g* for 10 min, the supernatant was transferred to a clean tube, and the pellet was re-extracted with 200 μL of 70% methanol. After centrifugation, both supernatants were combined and filtered through a 0.45-μm membrane (Ultrafree MC Duropore, Millipore). Extracts were subjected to HPLC using a reverse-phase C_{18}, ODS 2, 5-μm 250 × 4.6 mm column (PhaseSep, Clwyd, UK) protected by a Guard-Pak precolumn (Waters, Millipore) containing Resolve C_{18} (Waters). Sample injection was by a Rheodyne (Berkeley, CA) valve fitted with a 20-μL loop. Detection of lettucenin A was by fluorescence using a Shimadzu (Tokyo, Japan) RF535 detector set at 440-nm excitation and 515-nm emission wavelengths. Separation of lettucenin A was achieved at a column temperature of 40°C under isocratic conditions using water:acetonitrile (60:40) and a flow rate of 1.5 mL min^{-1}. For quantification of lettucenin A, standard solutions were prepared in methanol using the published extinction coefficient at the wavelength at maximum absorbance, 446 nm (Takasugi et al., 1985).

Transmission EM

Small pieces of leaf tissue (10 mm × 5 mm) were quickly excised and placed on dental wax under a drop of cold fixative (4°C). The sample was then cut into approximately 2-mm^2 pieces using a new razor blade and fixed in 2.5% (v/v) glutaraldehyde in 50 mM Pipes buffer at pH 7.2 for 12 h at 4°C. After fixation, samples were washed in Pipes (10 min, three times) and postfixed in 2% (v/v) osmium tetroxide in Pipes buffer for 2 h. Samples were again washed in Pipes (10 min, three times) and then dehydrated in a graded series of increasing acetone concentrations (50, 70, 80, and 90% [v/v] acetone, 10 min each incubation, followed by three changes of 100% acetone of 20-min duration each). Dehydrated samples were progressively embedded in Epon-Araldite at 3:1 acetone:resin, 15 min; 2:1 acetone:resin, 12 h; 1:1 acetone:resin, 15 min; 1:2 acetone:resin, 15 min; 1:3 acetone:resin, 15 min; fresh resin, 24 h, followed by a further change of fresh resin for 4 h.

Embedded samples were transferred to blocks in fresh resin and polymerized at 60°C for 48 h. Ultrathin sections (70–90 nm) were cut using a diamond knife (Diatome, Bienne, Switzerland) on a Reichert (Milton Keynes, UK) Ultracut E ultramicrotome and mounted on uncoated copper grids (300 mesh). Sections were stained in uranyl acetate/lead citrate (Brown and Mansfield, 1988) and examined using an Hitachi H7000 transmission electron microscope at accelerating voltages of 50 and 75 KV.

Histochemistry, Cytochemistry, and Immunocytochemistry

Phenolics

Localization of phenolic compounds at the ultrastructural level was carried out essentially as described by Brisson et al. (1977). Tissue samples were trimmed under a drop of cold (4°C) 2.5% (v/v) glutaraldehyde and fixed in a solution of 2.5% (v/v) glutaraldehyde containing 3% (w/v) freshly dissolved $FeCl_3$. Samples were fixed for 5 h, washed in 50 mM Pipes buffer at pH 7.0, and then washed in distilled water. Postfixation in osmium was omitted and the samples were subsequently processed as previously described. As a control, tissue was fixed in the absence of $FeCl_3$.

Localization of Hyp-Rich Glycoproteins

Tissues were fixed in 2.5% (v/v) formaldehyde in 50 mM Pipes buffer, pH 7.2, for 16 h at 4°C, then washed in Pipes (5 min, three times) and distilled water (5 min, two times). Postfixation in osmium was omitted and samples were dehydrated in a graded ethanol series (30, 50, 70, and 90% ethanol, 10 min each change, followed by three changes of 100% ethanol, 10 min each change). Samples were then progressively embedded in LR white resin (London Resin Co., London, UK) medium grade (1:1 resin:ethanol, 60 min; 3:1 resin:ethanol, 60 min; fresh resin 12 h, followed by a further change of fresh resin for 8 h). Samples were then placed in embedding capsules, fresh resin was added, and air was excluded. Polymerization was undertaken at 60°C for 24 h. Sections from polymerized blocks were mounted on uncoated gold grids (300 mesh).

For immunogold localization, all solutions were prepared in TBST. Sections to be labeled with anti-melon

$HRGP_{2b}$ were blocked in 2% (w/v) BSA in TBST for 30 min at room temperature and then transferred to a 20-μL droplet of the primary antiserum, rabbit anti-melon $HRGP_{2b}$. The rabbit polyclonal antiserum, raised to glycosylated melon $HRGP_{2b}$ (Mazau et al., 1988) and purified melon $HRGP_{2b}$, was kindly provided by Drs. D. Rumeau and M.-T. Esquerré-Tugayé (Université Paul Sabatier, Toulouse Cedex, France). Sections were treated with anti-$HRGP_{2b}$ diluted 1:100 and 1:500 and incubated for 16 h at 4°C. After they were washed in a stream of TBST from a wash bottle, grids were incubated in goat anti-rabbit antibody conjugated with 10-nm gold IgG (Amersham or Sigma), diluted 1:25 in TBST, for 30 min at room temperature. Grids were subsequently washed in a stream of TBST and then in a stream of distilled water. Sections were dried and examined without further treatment.

Controls for the specificity of immunogold labeling were incubation in the absence of the primary antibody, replacement of the immune serum by nonimmune rabbit serum (because no preimmune serum was available), and preabsorption of antiserum with pure $HRGP_{2b}$. For preabsorption, 20 μL of pure melon HRGP (100 μg mL^{-1}) was added to 20 μL of a 1:50 dilution of anti-$HRGP_{2b}$ and the solutions were incubated at room temperature for 2 h.

Callose

Semithin sections (1 μm) of LR white-embedded tissue were cut and mounted on glass slides. A 20-μL droplet of aqueous aniline blue (0.05%, w/v) in 50 mM phosphate buffer, pH 8.0, was added to the section and a coverslip was placed over it. The section was immediately viewed under UV excitation, with a bright, light-blue fluorescence being indicative of callose (O'Brien and McCully, 1981).

RESULTS

Physiological Characterization of Responses to Wild-Type and Hrp⁻ Strains

Macroscopic Symptoms and Membrane Damage

The first sign of response to either strain was observed 5 h after inoculation as the appearance of faint glazing of the abaxial leaf surface. At sites inoculated with S21-WT, glazing became confluent after 6 h, areas of tissue collapse were observed after 8 h, and after 15 h the zone of infiltrated tissue was completely collapsed and desiccated. The HR lesion had become characteristically brown and papery 1 d after inoculation. The glazing caused by S21–533 was transient and had disappeared by 12 h after inoculation, when infiltrated zones were indistinguishable from healthy uninoculated tissue. No symptoms were observed after injection with water alone. Collapse of tissue during the HR was associated with a loss in fresh weight (data not shown).

Because cell collapse was visible 8 h after inoculation with S21-WT, studies on membrane integrity were confined to the first 12 h of the interaction. Two parameters were used, the direct measurement of cells that failed to plasmolyze (Woods et al., 1988) and electrolyte leakage from infiltrated tissue (Croft et al., 1990). Significant differences between S21-WT and S21–533 were first detected using the sensitive plasmolysis technique (Fig. 1A). More than 50% of lettuce cells failed to plasmolyze by 8 h after inoculation with S21-WT. It is interesting that failure to plasmolyze was also detected in a few cells after inoculation with S21–533. Some cells (up to 10% in certain samples) also appeared to have failed to plasmolyze after infiltration with water, indicating the level of "false positives" observed due to the examination of thin sections. As shown in Figure 1B, the increasing number of cells failing to plasmolyze after inoculation with S21-WT was correlated

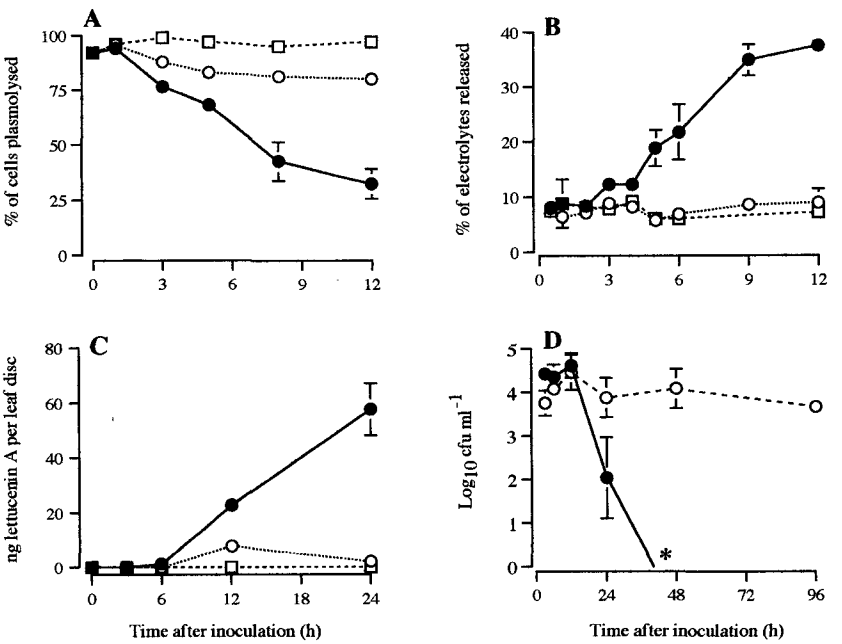

Figure 1. Characterization of responses to wild-type and Hrp⁻ strains. A and B, Detection of membrane damage. A, Numbers of cells that retain the ability to plasmolyze within inoculated tissues. Tissues were plasmolyzed in 0.8 M KNO_3 prior to fixation and embedding for conventional EM. Data presented as mean ± SE from eight separate experiments. A minimum of 500 cells was assessed for plasmolysis within each experiment. B, Electrolyte leakage from inoculated tissues. Data are the means ± SE from three experiments. C, Phytoalexin accumulation. Levels of lettucenin A accumulation within inoculated tissues are presented as mean ± SE of three independent extractions. D, Bacterial multiplication. Data for the recovery of bacteria from inoculated tissues are presented as mean ± SE from three separate experiments. *, Failure to recover bacteria at this time point. ●, S21-WT; ○, S21–533; □, SDW.

with a progressive increase in electrolyte leakage from 5 h after inoculation. No increases in electrolyte leakage were detected in tissues inoculated with S21–533.

Phytoalexin Accumulation

Yields of lettucenin A are given in Figure 1C based on the area of leaf tissue extracted rather than fresh weight because of the desiccation observed during the HR. A trace of lettucenin A was detected in tissue inoculated with S21-WT 6 h after infiltration. At this time some mesophyll cells had already failed to plasmolyze. As reported by Bennett et al. (1994), the phytoalexin subsequently increased rapidly in concentration within tissue undergoing the HR but was not detected outside the lesion. A significant accumulation of lettucenin A was detected within macroscopically symptomless tissue 12 h after inoculation with the Hrp$^-$ strain, but levels decreased between 12 and 24 h.

Bacterial Multiplication

Data on the recovery of bacteria from inoculated tissue are given in Figure 1D. Neither strain multiplied significantly. After the collapse of tissue during the HR, no cfus of S21-WT were recovered. These results indicated that the HR had generated bacteriocidal conditions, whereas Hrp$^-$ bacteria remained in a state of bacteriostasis.

Microscopical Studies

It was clear from the physiological and biochemical characterization of reactions that the *hrpD* mutant, although failing to cause lasting macroscopic symptoms, did cause responses at the cellular level and some phytoalexin accumulation. Microscopy allowed reactions occurring within individual cells and at micro-sites containing bacterial colonies to be examined in detail. The typical appearance of a cell junction in noninoculated tissue or leaves infiltrated with water alone is shown in Figure 2. Organelles and membranes were well preserved after the fixation and embedding procedures used.

Quantitative Analyses of Major Responses

Preliminary examination of tissue fixed at 12 and 24 h after inoculation revealed that two major responses occurred (as illustrated in Fig. 3). Both the wild-type and Hrp$^-$ strains induced the formation of strikingly large papillae adjacent to sites of bacterial attachment to the plant cell wall. In addition, the wild-type strain S21-WT caused complete cytoplasmic collapse. Quantitative time-course analyses (summarized in Fig. 4) confirmed that the major differences between strains were the generally more rapid deposition of papillae in response to S21-WT and the almost complete absence of tonoplast rupture and loss of compartmentation in cells next to the Hrp$^-$ S21–533. The high frequency of occurrence of cell wall alterations and (in the case of S21-WT) cytoplasmic collapse allowed the development of each response to be examined in detail.

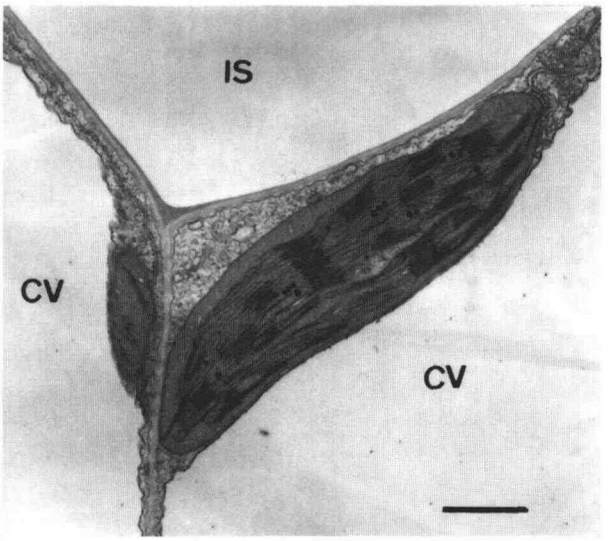

Figure 2. A mesophyll cell junction within tissue prior to inoculation. Note that the plasma membrane appears closely associated with the cell wall and that a large central vacuole is bordered by an intact tonoplast. Peripheral cytoplasm contains well-preserved chloroplasts. Bar = 1 μm. IS, Intercellular space; CV, central vacuole.

Cell Wall Alterations

The same pattern of papilla deposition was observed in cells adjacent to Hrp$^-$ or wild-type bacteria. The ultrastructural changes observed are, therefore, illustrated in Figures 5 and 6 using examples selected from both interactions.

The first response was the apparent convolution of the plasma membrane next to bacterial cells, and by 3 to 5 h after inoculation, the accumulation of lightly stained fibrillar material was observed between the convoluted membrane and the plant cell wall (Fig. 5). Between 3 and 8 h progressive thickening and increase in complexity of the paramural deposits occurred. The fibrillar matrix was enlarged and became impregnated with numerous osmiophilic and vesicular particles (Fig. 6, A and B). In many cases the complex paramural deposits filled large areas of the cell (Fig. 6A). Fixation of inoculated tissue under hypertonic conditions showed that the plasma membrane could be detached from developing deposits during plasmolysis, as shown in Figure 6B.

Initial deposition of fibrillar material was not associated with major changes in the cytoplasm of responding cells. As papillae developed, however, distinct proliferation and swelling of the ER was observed in the majority of challenged cells. Smooth vesicles and MVBs were commonly observed within the cytoplasm at sites of deposit formation. Figure 6C shows that the small vesicles within the MVBs resembled the vesicle-like structures found within paramural deposits. In some sections the outer membrane of MVBs appeared to fuse with the plasma membrane, discharging vesicles into the paramural space. As deposits increased in complexity, an electron-translucent material

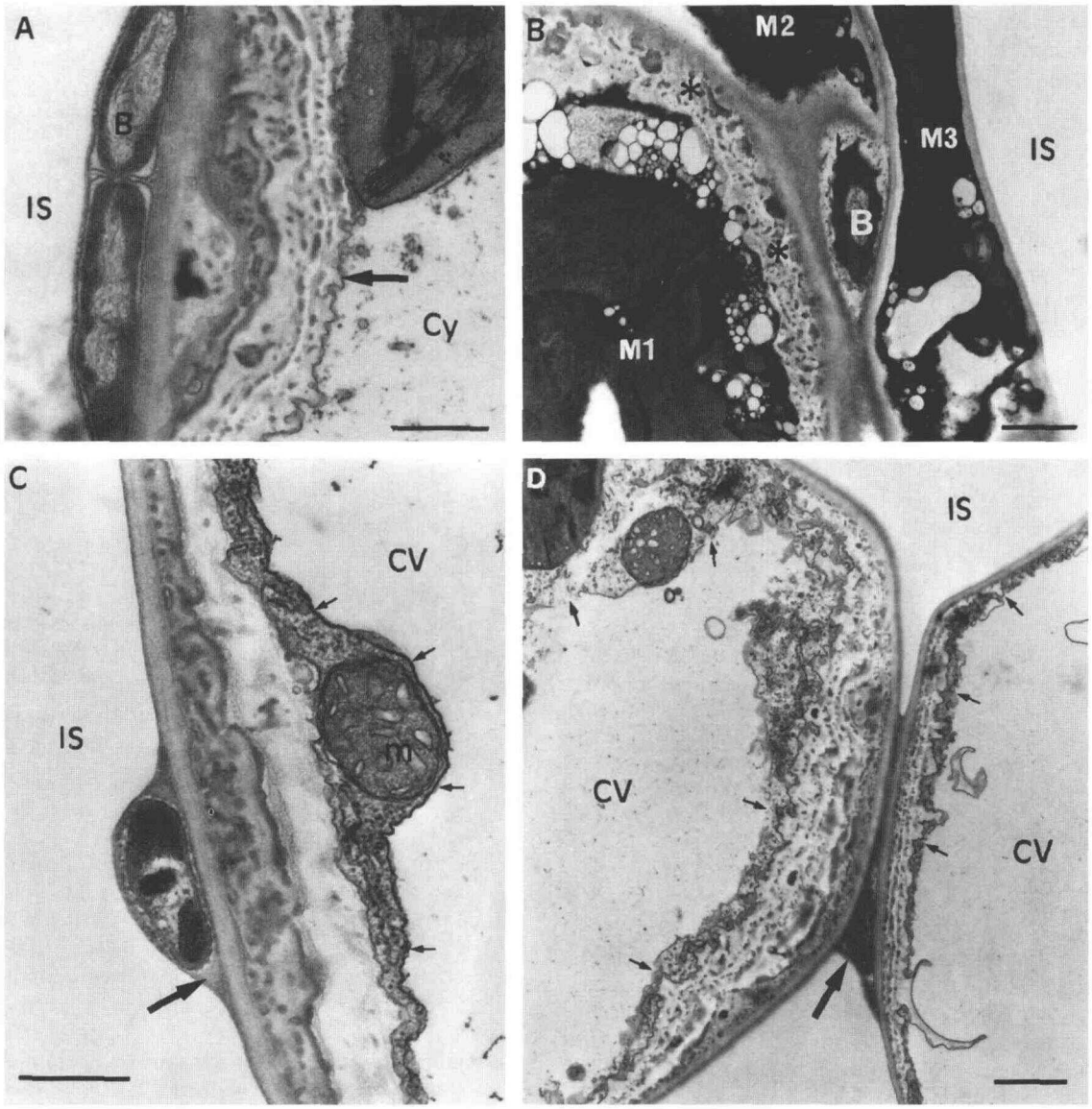

Figure 3. Late stages of papilla development and cell collapse. A, Cells of S21-WT located at the wall of a collapsed mesophyll cell 12 h after inoculation. The large paramural deposit (arrow) remains distinctly layered. Note that the chloroplast retains remarkable ultrastructural integrity, even though the cytoplasm has degenerated. Bar = 0.5 μm. B, Detail of mesophyll cells (M1, M2, and M3) 24 h after inoculation with S21-WT. All three mesophyll cells have collapsed around the bacterium and contain a condensed cytoplasm; no central vacuoles are present. The edge of the condensed cytoplasm of M1 is vacuolated and a layered paramural deposit lines the cell wall (asterisk). Paramural deposits are not visible in M2 or M3. Bar = 1 μm. C, Cell of Hrp⁻ S21–533 located on a mesophyll cell wall 12 h after inoculation. A large, complex, layered paramural deposit is located at the site of bacterial attachment. The bacterial cell is encapsulated by material continuous with the plant cell wall (large arrow). Note that the mitochondrion appears well preserved and that the tonoplast is intact (small arrows). Bar = 0.5 μm. D, Late stage of papilla formation next to cells challenged by S21–533 24 h after inoculation. The mesophyll cells contain large and extensive paramural deposits. Deposits are thickest at the point opposite bacterial attachment to the cell wall (large arrow). Although an intact mitochondrion is visible, there is a lack of tonoplast continuity (small arrows), suggesting that irreversible membrane damage has occurred. Bar = 1 μm. B, Bacterium; Cy, degenerate cytoplasm; IS, intercellular space; m, mitochondrion; CV, central vacuole.

appeared to cover the fibrillar matrix, which contained layers of irregularly shaped, osmiophilic particles and vesicles (Fig. 3A).

In addition to the deposition of material next to the plasma membrane, an amorphous electron-dense matrix, apparently continuous with the plant cell wall, accumulated around bacterial cells (Figs. 3, 5, and 6; see also "Cytoplasmic Collapse"). By 12 h after inoculation, bacteria at many sites had become embedded in encapsulating material. In agreement with data obtained from population counts, the numbers of bacteria within colonies remained low, usually one or two bacteria at each site.

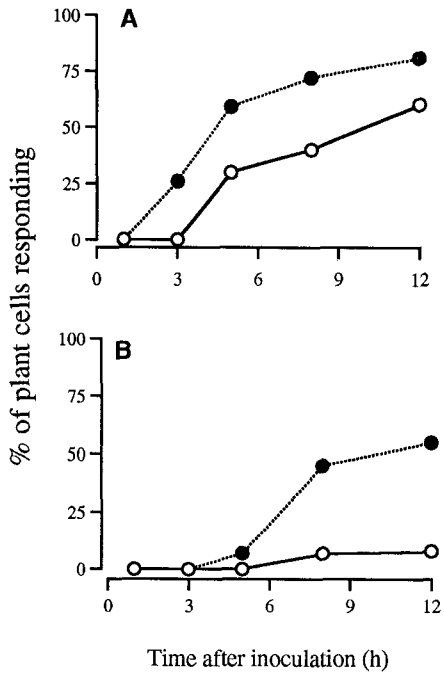

Figure 4. Quantitative assessment of ultrastructural responses of lettuce cells to bacterial challenge. A, Formation of papillae more than 0.2 μm thick. B, Cytoplasmic disorganization, indicated by tonoplast rupture and dispersal of organelles in the vacuolar space. A minimum of 50 sites of bacteria-plant cell attachment was assessed at each time point. ●, S21-WT; ○, S21–533.

Immunocytochemical and Histochemical Analysis of Deposits

Polyclonal antiserum raised against the melon $HRGP_{2b}$ (Mazau and Esquerré-Tugayé, 1986; Mazau et al., 1988) was used to localize the glycoproteins in lettuce mesophyll tissue. On sections of uninoculated or water-infiltrated leaves, gold labeling was sparse but most common on the inner face of the cell wall and in regions of cytoplasm close to the wall. By 3 h after inoculation with S21-WT or S21–533, there was a striking increase in the density of label in the cell wall next to bacterial colonies. Gold label was also clearly associated with paramural deposits and material surrounding the bacteria (Fig. 7, A–C). Increases in density of labeling were initially most marked after inoculation with S21-WT. Paramural deposits became heavily labeled, but, at sites with well-formed papillae, labeling within the material encapsulating bacteria and also the wall itself was less frequent. No immunogold labeling was observed with nonimmune antisera or with anti-$HRGP_{2b}$ antibodies after their adsorption to purified melon HRGP (Fig. 7D).

Deposition of phenolics was examined at the ultrastructural level by $FeCl_3$ staining, which revealed the presence of phenolic material within papillae. Examination of sections of noninoculated tissue stained with $FeCl_3$ revealed an electron-dense cytoplasm but no staining along the cell wall or within organelles. By contrast, dark, electron-dense deposits were observed within paramural deposits. At some sites, the electron-dense regions formed distinct layers, as illustrated in Figure 8A. Within papillae, material staining positively for phenolics appeared to be distributed in a manner corresponding to that of the vesicles detected using conventional staining (see Fig. 6). The ER was also clearly delineated as an electron-dense structure within tissue inoculated with both S21-WT and S21–533, indicating sites of phenolic synthesis. Nonosmicated tissue, fixed in the absence of $FeCl_3$, had neither an electron-dense ER nor dense deposits in regions of paramural deposition.

Callose was commonly detected within papillae using the aniline blue-induced fluorescence technique by 5 and 8 h after inoculation with S21-WT and S21–533, respectively (Fig. 8B). The timing and frequency of detection of callose by fluorescence corresponded to the appearance of electron-translucent layers within deposits (Fig. 3A).

Overall, the histochemical studies indicated that the earliest deposits contained HRGPs and that the initial matrix became impregnated with phenolics and, finally, callose.

Cytoplasmic Collapse

In addition to reactions associated with localized papilla deposition, progressive vacuolation and organelle disruption occurred within the cytoplasm of cells adjacent to colonies of S21-WT (Figs. 3B and 9). The appearance of numerous small vacuoles throughout the cytoplasm, as shown in Figure 9B, appeared to precede tonoplast rupture and cytoplasmic disorganization. However, the speed of transition from a vacuolated cytoplasm containing recognizable organelles to a disorganized, electron-dense aggregate (Figs. 3B and 9C) was quite variable. Dysfunction of the plasma membrane clearly preceded tonoplast rupture, since many cells that failed to plasmolyze retained an intact, large, central vacuole. It is interesting that within partially collapsed cells, chloroplasts often retained structural integrity (Fig. 3A). By contrast, mitochondria seemed particularly sensitive, and even 3 h after inoculation with the wild-type strain many examples of swelling and poor preservation of the internal membranes were seen before any other degenerative changes had occurred (Figs. 5B and 6, A and B). Time-course studies suggested that localized deposition of papillae continued during the phase of vacuolation, but deposits often became dispersed in cells after tonoplast failure.

DISCUSSION

Microscopy has revealed two distinct responses of lettuce cells to *P.s.* pv *phaseolicola*: (a) localized cell wall alterations, including papilla deposition, and (b) membrane damage leading to cytoplasmic collapse and the macroscopic appearance of the HR. Signals for both responses were delivered by the wild-type strain, but the *hrpD* mutant typically induced only the very localized wall changes that were a striking feature of both interactions.

Appositions acquired a progressively more complex structure during the time course. During exocytosis, ER-located products, destined for extracellular secretion, are generally thought to pass through the Golgi apparatus, and Golgi-derived vesicles traffic cell wall components to the plasma membrane (Delmer and Stone, 1988; Battey and

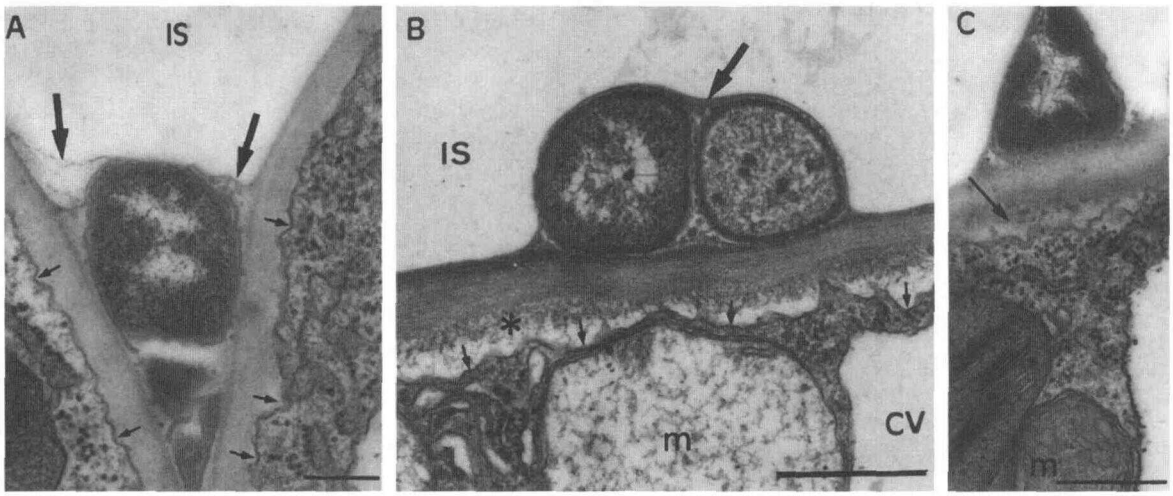

Figure 5. Early responses. A, Cell of Hrp⁻ S21–533 located at a mesophyll cell junction 3 h after inoculation. The plasma membrane is slightly convoluted (small arrows) in proximity to the bacterium, and limited deposits of fibrillar material can be observed interspersed between the membrane and the cell wall. The bacterium is surrounded by a loose layer of material (large arrow) continuous with the extracellular surface of the cell wall. Bar = 0.25 μm. B, Cells of S21-WT attached and encapsulated (large arrow) on a mesophyll cell wall 3 h after inoculation. The plasma membrane is extensively convoluted (small arrows), and a lightly stained, fibrillar material (asterisk) is located between the membrane and the cell wall. Note that the mitochondrion lacks well-preserved cristae. Bar = 0.5 μm. C, Cell of Hrp⁻ S21–533 attached to a mesophyll cell wall 8 h after inoculation. A distinct, layered papilla (arrow), containing osmiophilic particles in addition to fibrillar material, has developed at the site of bacterial attachment to the plant cell wall. Again, the bacterium is encapsulated by wall-like material. A well-preserved mitochondrion is visible within the cytoplasm. Bar = 0.5 μm. m, Mitochondrion; IS, intercellular space; CV, central vacuole.

Blackbourn, 1993; Driouich et al., 1993). Swelling of the ER and an increase in numbers of variously sized, smooth vesicles were observed at sites of paramural deposition. In addition, MVBs were observed only in cells with deposits, and some of the vesicle-like structures within paramural deposits appeared to originate from MVBs. It is not clear whether MVBs are involved in exocytotic or endocytotic events; they may be involved in the removal and disposal, in the central vacuole, of components of the periplasmic matrix (Herman and Lamb, 1992). Elicitor molecules may also be endocytosed into the cell (Bolwell et al., 1991; Horn et al., 1992). Nevertheless, the progressive increase in size of paramural deposits suggests an exocytotic role for most of the vesicles. Calcium has been shown to be important in the regulation of vesicle fusion and exocytosis in plant cells (Bolwell, 1988; Battey and Blackbourn, 1993), but the temporal and spatial control of the directed secretion identified in lettuce remains to be determined. Papillae became most highly developed in the absence of cell collapse. By contrast, the progressive loss of compartmentalization and cytoskeletal integrity probably accounts for the more widespread deposition observed in many cells during the later stages of the HR.

Immunocytochemical studies indicated that the earliest changes in the cell wall adjacent to bacteria involved the incorporation of HRGPs. Benhamou et al. (1991) consider that the major epitopes recognized by the $HRGP_{2b}$ antiserum are on the polypeptide moiety of the molecule. The accumulation of HRGPs within deposits and cell walls prior to the detection of phenolic compounds at these sites is consistent with their proposed role in providing nucleation sites for lignin-like polymer deposition (Whitmore, 1978). HRGPs may also interact ionically with other wall components. Negatively charged uronic acid residues of pectin are possible sites of interaction with positively charged HRGP (Showalter and Varner, 1989), and Qi and Mort (1990) have suggested that there may be HRGP cross-linking sites in pectin. Such interactions may explain the loss of labeling in the cell wall at later stages in the time course as epitopes are masked by the deposition of additional material or through interactions with other wall components.

After their incorporation into cell walls, HRGPs are rapidly insolubilized (Cooper and Varner, 1983). Rapid insolubilization of pre-existing Pro-rich plant cell wall protein and a putative HRGP after treatment of soybean cells with elicitor preparations was reported by Bradley et al. (1992). Insolubilization has been proposed to be the result of the formation of intermolecular isodityrosine cross-links mediated by a specific peroxidase/H_2O_2 system (Fry, 1986; Everdeen et al., 1988; Brownleader et al., 1993). The polymerization of phenolics within the wall is also believed to result from peroxidase activity (Hahlbrock and Scheel, 1989; Graham and Graham, 1991; Bolwell, 1993), which, initially, must be highly localized within lettuce cells adjacent to bacterial colonies. The H_2O_2 required for cross-linking reactions may result from NAD(P)H oxidation by peroxidase itself (Gross et al., 1977; Halliwell, 1978; Mäder and Amberg-Fisher, 1982). It is possible that peroxidase activity may also contribute to the increase in activated oxygen species during the HR (Vianello and Macri, 1991; Vera-Estrella et al., 1992; Mehdy, 1994). The potentially

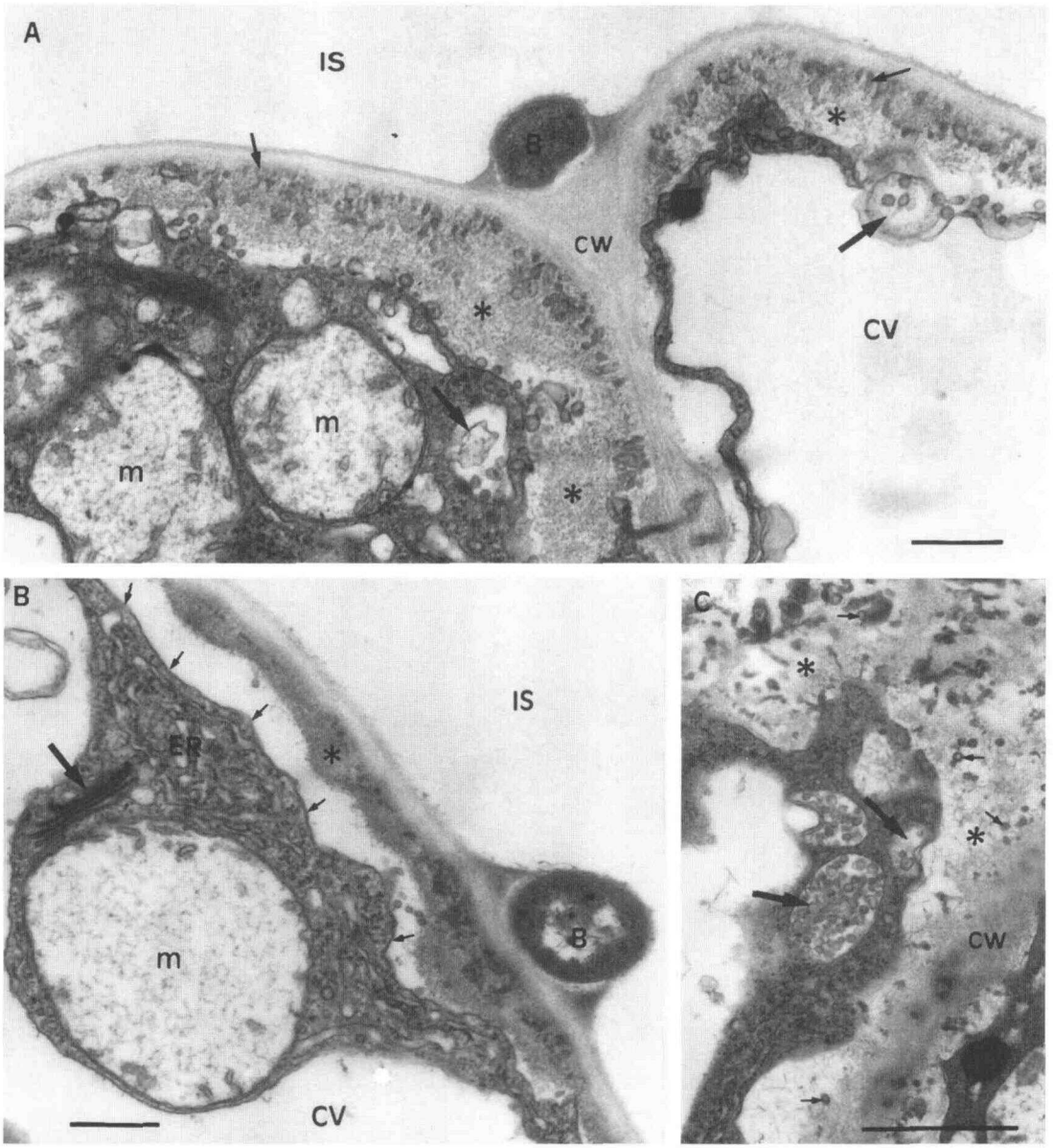

Figure 6. Development of paramural papillae. A, Cell of S21-WT located at a mesophyll cell junction 5 h after inoculation. Extensive paramural deposits have already developed (asterisks). Note the granular and vesicular deposits along the wall in both mesophyll cells (small arrows). The bacterium is surrounded by amorphous material. Mitochondria appear swollen, and smooth vesicles and MVBs (large arrows) are present at sites of deposition. Bar = 0.5 μm. B, Papilla formation 5 h after inoculation with S21-WT. The mesophyll cell was partially plasmolyzed during fixation, illustrating the lack of adhesion between the plasma membrane (small arrows) and paramural deposit (asterisk). Note the swollen mitochondrion, proliferation of ER, and the associated Golgi body (large arrow). Bar = 0.5 μm. C, Detail of the cytoplasm adjacent to sites of paramural deposition (asterisks). Vesicles and MVBs (large arrows) are shown apparently fusing with both tonoplast and plasma membrane. The MVBs contain vesicle-like structures that resemble those observed within the papillae (small arrows). Bar = 0.5 μm. B, Bacterium; CW, plant cell wall; IS, intercellular space; m, mitochondrion; CV, central vacuole.

dual role of peroxidase in the formation of wall alterations and also generation of H_2O_2 leading to the HR in lettuce merits detailed investigation. Analysis of peroxidase activities using ultrastructural techniques will be needed to resolve the subcellular regulation of reactions observed.

Characteristic morphological changes, including degeneration of the nucleus and fragmentation of the cytoplasm into several large membrane-bound vesicles, are associated with apoptotic cell death in animal cells (Sen, 1992; Martin et al., 1994). A very different sequence of ultrastructural events was involved in the collapse of lettuce cells during the HR. The earliest responses observed were mitochondrial swelling and lack of preservation of cristae. Changes in mitochondrial structure appeared to be followed by

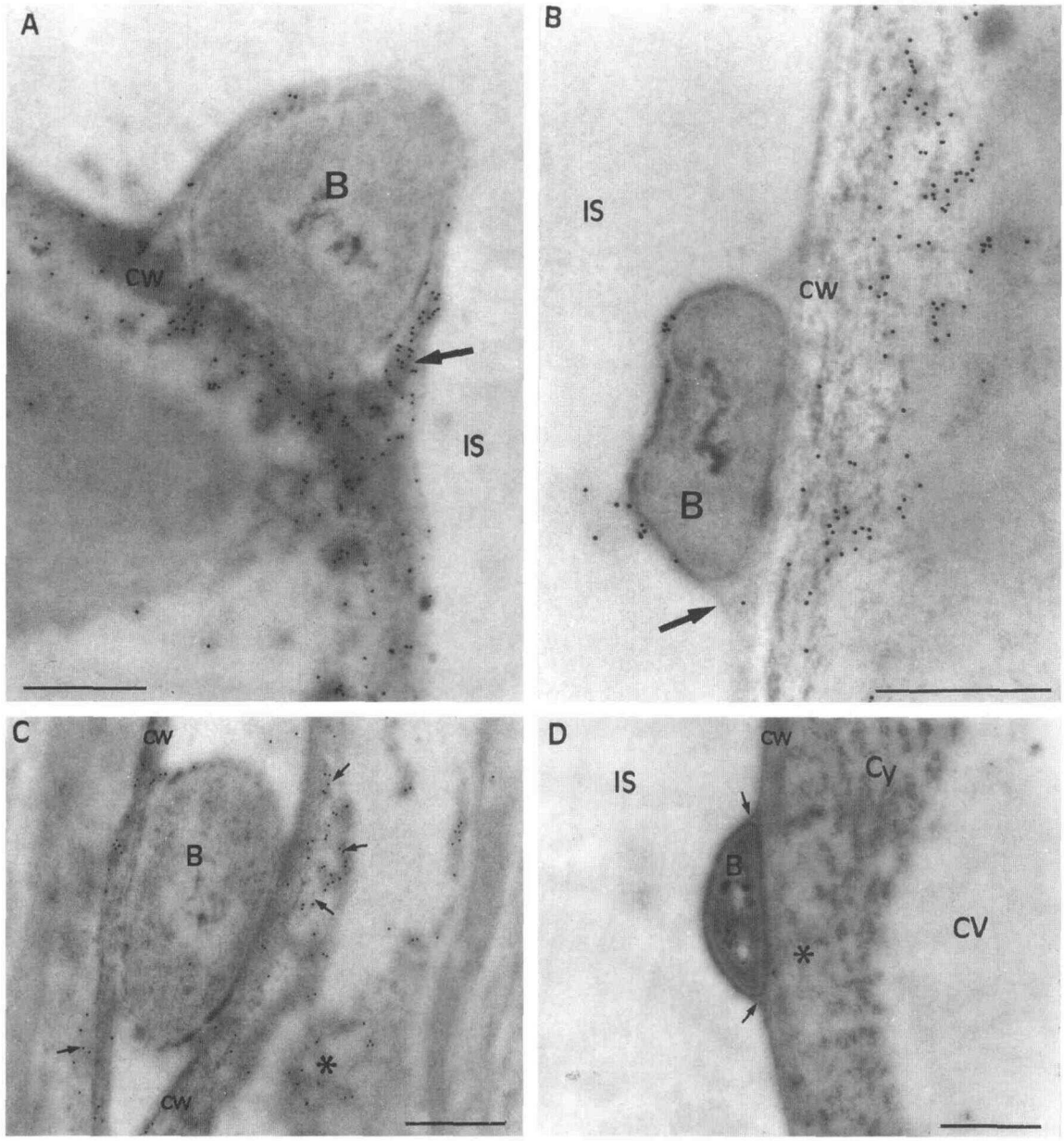

Figure 7. Immunocytochemical localization of HRGPs within papillae. Five (A) and 8 (B) h after inoculation with S21-WT. Note that papillae are densely labeled and that labeling in the wall per se and encapsulating material (arrow) is greater at the earlier time point. Bars = 0.25 μm and 0.5 μm, respectively. C, Hrp⁻ S21–533 located at a mesophyll cell junction 8 h after inoculation. Small papillae (arrows) and the plant cell wall are labeled. Untypically, at this site there is also label within the aggregated cytoplasm (asterisk). Bar = 0.5 μm. D, Cell of S21-WT attached to a mesophyll cell wall 5 h after inoculation. The section was incubated in immune serum that had been preabsorbed with purified melon HRGP prior to incubation in the gold-conjugated secondary antiserum. Note the absence of label from the cell wall, encapsulating material (arrows), and site of papilla formation (asterisk). Bar = 0.5 μm. B, Bacterium; CV, central vacuole; cw, plant cell wall; Cy, cytoplasm; IS, intercellular space.

plasma membrane dysfunction (indicated by failure to plasmolyze), which led to the progressive vacuolation of the cytoplasm, general organelle disruption, and tonoplast collapse. The HR occurring in lettuce is more closely comparable to the process of necrosis in animal cells, in which the critical event is cell membrane damage (Buja et al., 1993).

Although the extent of localized cell wall alterations, including HRGP, phenolics, and callose deposition, was very similar in response to S21-WT and S21–533, accumulation of the phytoalexin lettucenin A was very different. Our observations suggest that there is a close link between the occurrence of irreversible membrane damage and induction of phytoalexin synthesis. A threshold level of

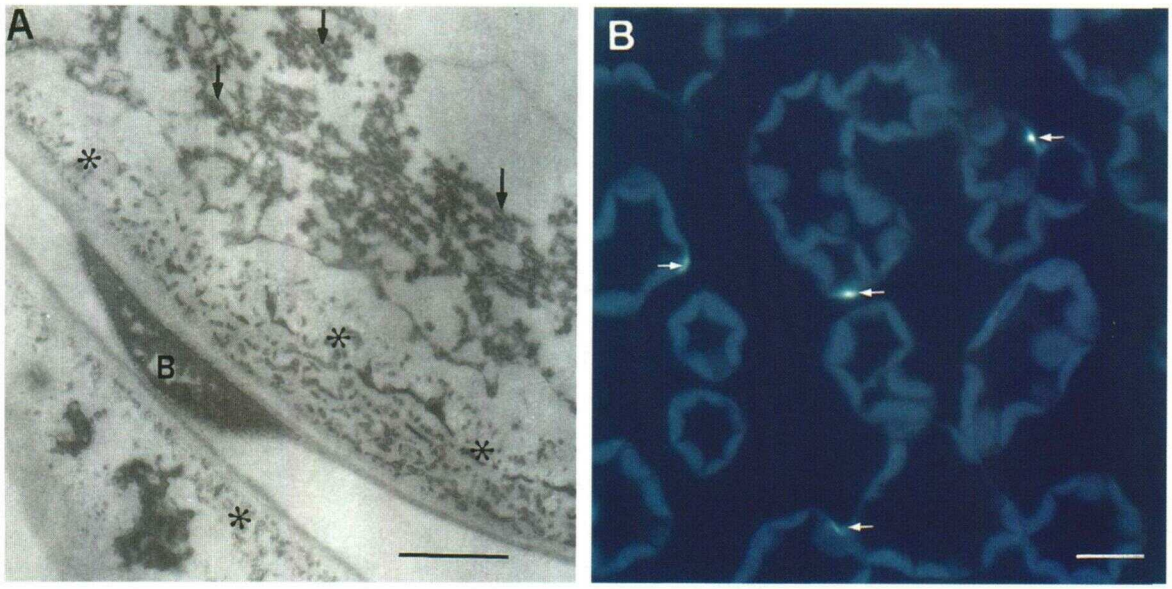

Figure 8. Localization of phenolics and callose within papillae. A, Detection of phenolics within papillae (asterisk) and ER (arrow) 8 h after inoculation with S21-WT. Note the layers of $FeCl_3$-stained material opposite the bacterial cell. Bar = 1 μm; B, bacterium. B, Deposits (arrow) in tissue fixed 8 h after inoculation with S21–533 show characteristic fluorescence of β-1,3-glucan after staining with aqueous aniline blue. Bar = 10 μm.

membrane dysfunction may be essential for the release of endogenous elicitors that trigger lettucenin A biosynthesis. The very low number of dead cells observed in response to S21–533 was reflected by a limited increase in phytoalexin production. The death of isolated cells in response to Hrp mutants, which would be detected only under the microscope, may occur in other plants. In bean, this may explain the increase in phytoalexins reported by Jakobek and Lindgren (1993) in macroscopically symptomless tissues infiltrated with Hrp^- bacteria. In lettuce, the very limited cytoplasmic collapse occurring in response to S21–533 was not associated with the rapid degenerative changes observed during the HR. The extensive deposition of papillae that may be associated with high concentrations of H_2O_2 and phenoxy radicals (Campa, 1991) may occasionally be so great as to lead to cell death.

Hrp^- strains of bacteria have been reported characteristically to fail to multiply within plants. Our observations, in agreement with those of Jakobek and Lindgren (1993), suggest that rather than Hrp^- bacteria simply being unable to take up nutrients from the intercellular space, their growth may be actively inhibited by defense responses that do not involve the HR. An obvious candidate as a mechanism for the restriction of bacterial multiplication in lettuce is the progressive encapsulation of cells in the HRGP-containing matrix, which appears to bind bacteria to the plant cell wall. Such encapsulation may render the bacteria susceptible to increases in H_2O_2 concentrations at sites of papilla formation (Peng and Kuć, 1992) and, particularly in the interaction with S21-WT, to localized increases in the concentration of lettucenin A. The intracellular nature of the complex paramural deposits produced suggests that they may not exert a direct effect on bacterial multiplication within intercellular spaces. However, the resulting hydrophobicity imparted after the potential lignification of host cell walls may serve to restrict the diffusion of microbial metabolites to the host and the diffusion of host-derived nutrients to the pathogen as discussed by Vance et al. (1980), Friend (1981), and O'Connell et al. (1990).

It has been proposed that Hrp proteins form a secretory apparatus that may be involved in the export of elicitors of the HR and determinants of pathogenicity (Fenselau et al., 1992; He et al., 1993). It is possible that the membrane-associated HrpD protein (Miller et al., 1993) may contribute to an export pathway in *P.s.* pv *phaseolicola* and that the failure of S21–533 to induce the HR is due to an inability to deliver the appropriate signal. It is clear that the Hrp^- strain is able to deliver an unknown factor that must, directly or indirectly, traverse the cell wall and activate formation of complex wall alterations, including the highly localized deposition of HRGPs, callose, and phenolics in lettuce cells. Whether or not mutants defective at other *hrp* loci or, indeed, saprophytic bacteria are also able to induce such localized wall alterations in lettuce remains to be determined. Although encapsulation has been observed as a general response to bacteria in a number of interactions (Pueppke, 1984), studies in bean have shown that saprophytes lack the ability to induce complex papilla formation (Brown and Mansfield, 1988).

Paradoxically, although the formation of paramural deposits and encapsulation may serve to prevent bacterial multiplication, the failure of S21–533 to elicit the HR means that the *hrpD* mutant survives within the nonhost tissue, whereas wild-type bacteria are eliminated. It seems probable that the accumulation of the highly toxic lettucenin A and tissue desiccation during the HR may generate a bacteriocidal environment. In the interaction between *P.s.* pv *phaseolicola* and the nonhost lettuce it would seem advan-

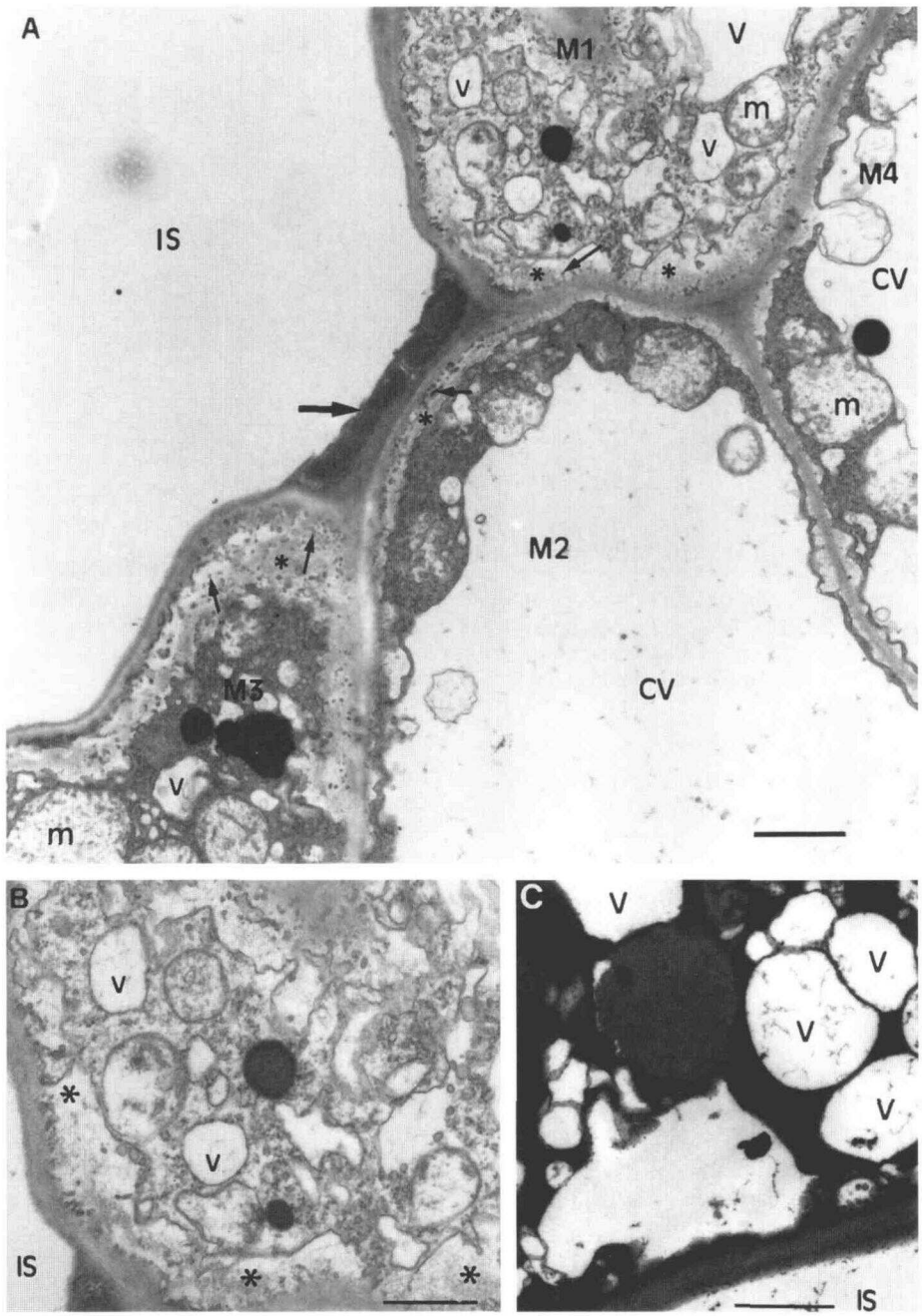

Figure 9. Cytoplasmic disorganization in response to S21-WT. A, Cells of S21-WT (large arrow) bordered by three mesophyll cells (M1, M2, and M3) fixed 12 h after inoculation. Large and extensive paramural deposits are present within the cells immediately adjacent to the bacteria. The deposits comprise osmiophilic particles (small arrows) within a lightly stained matrix (asterisk) and have a layered appearance that is most clearly defined in M2 and M3. The cytoplasm of M1 and M3 is extensively vacuolated, and mitochondria are disrupted, although the tonoplast appears to be intact. Mesophyll cell M4 also shows evidence of paramural deposition, invaginations of the plasma membrane, and mitochondrial disruption. The bacteria are darkly stained and embedded in an electron-dense matrix. Bar = 1 μm. B, Detail of M1 showing extensive vacuolation of the cytoplasm and evidence of organelle disruption. The paramural deposit (asterisks) appears dispersed. Bar = 0.5 μm. C, Detail of cell near completion of hypersensitive collapse. The vacuolated cytoplasm has developed into an electron-dense amorphous mass. Bar = 0.5 μm. B, Bacterium; IS, intercellular space; m, mitochondrion; CV, central vacuole; v, vacuolation.

tageous not to retain Hrp functions. The implied ability of Hrp^- strains of phytopathogens to survive in nonhost plant tissues in the absence of the HR may explain the frequent recovery of apparently saprophytic but related forms of bacteria from symptomless plants (E. Billing, unpublished observations). The possession of Hrp functions may be a positive disadvantage for a saprophytic existence.

ACKNOWLEDGMENTS

We wish to thank Ian Brown for critically reading the manuscript and Shelagh Reardon and Fiona Holt for advice concerning all aspects of light and electron microscopy. We also thank M. Nöllenburg for unpublished information concerning the location of the Tn5 insertion in S21–533.

Received November 29, 1994; accepted February 3, 1995.

LITERATURE CITED

Adám A, Farkas T, Somlyai G, Hevesi M, Király Z (1989) Consequence of O_2^- generation during bacterially induced hypersensitive reaction in tobacco: deterioration of membrane lipids. Physiol Mol Plant Pathol **34:** 13–26

Bailey JA (1982) Physiological and biochemical events associated with the expression of resistance to diseases. *In* RKS Wood, ed, Active Defense Mechanisms in Plants. Plenum Press, New York, pp 39–65

Baker CJ, Orlandi EW, Mock NM (1993) Harpin, an elicitor of the hypersensitive response in tobacco caused by *Erwinia amylovora*, elicits active oxygen production in suspension cells. Plant Physiol **102:** 1341–1344

Battey NH, Blackbourn HD (1993) The control of exocytosis in plant cells. New Phytol **125:** 307–338

Benhamou N, Mazau D, Grenier J, Esquerré-Tugayé M-T (1991) Time course study of the accumulation of hydroxyproline-rich glycoproteins in root cells of susceptible and resistant tomato plants infected by *Fusarium oxysporum* f. sp. *radicis-lycopersici*. Planta **184:** 196–208

Bennett MH, Gallagher MDS, Bestwick CS, Rossiter JT, Mansfield JW (1994) The phytoalexin response of lettuce to challenge by *Botrytis cinerea*, *Bremia lactucae* and *Pseudomonas syringae* pv. *phaseolicola*. Physiol Mol Plant Pathol **44:** 321–333

Bestwick CS, Mansfield JW (1992) Early events associated with non-host resistance of lettuce to *Pseudomonas syringae* pv. *phaseolicola*. *In* Proceedings 4th International Working Group on *Pseudomonas syringae* pathovars. Stamperia Granducale, Florence, Italy, pp 127–131

Bolwell GP (1988) Synthesis of cell wall components: aspects of control. Phytochemistry **27:** 1235–1253

Bolwell GP (1993) Dynamic aspects of the plant extracellular matrix. Int Rev Cytol **146:** 261–324

Bolwell GP, Coulson V, Rodgers MW, Murphy DL, Jones D (1991) Modulation of the elicitation response in cultured French bean cells and its implication for the mechanism of signal transduction. Phytochemistry **30:** 397–405

Bowles DJ (1990) Defense-related proteins in higher plants. Annu Rev Biochem **59:** 873–907

Bradley DJ, Kjellbom P, Lamb CJ (1992) Elicitor- and wound-induced oxidative cross-linking of a proline-rich plant cell wall protein: a novel, rapid defense response. Cell **70:** 21–30

Brisson JD, Peterson RL, Robb J, Rauser WE, Ellis BE (1977) Correlated phenolic histochemistry using light, transmission, and scanning electron microscopy, with examples taken from phytopathological problems. *In* Proceedings of the Workshop on Other Biological Applications of the SEM/TEM. IIT Research Institute, Chicago, IL, pp 667–676

Brown IR, Mansfield JW (1988) An ultrastructural study, including cytochemistry and quantitative analyses of the interactions between pseudomonads and leaves of *Phaseolus vulgaris* L. Physiol Mol Plant Pathol **33:** 351–376

Brown IR, Mansfield JW, Irlam I, Conrads-Strauch J, Bonas U (1993) Ultrastructure of interactions between *Xanthomonas campestris* pv. *vesicatoria* and pepper, including immunocytochemical localization of extracellular polysaccharides and the AvrBs3 protein. Mol Plant Microbe Interact **6:** 376–386

Brownleader M, Golden KD, Dey PM (1993) An inhibitor of extensin peroxidase in cultured tomato cells. Phytochemistry **33:** 755–758

Buja M, Eigenbrodt ML, Eigenbrodt MD (1993) Apoptosis and necrosis. Basic types and mechanisms of cell death. Arch Pathol Lab Med **117:** 1208–1214

Campa A (1991) Biological roles of plant peroxidases: known and potential function. *In* J Everse J, MB Grisham, eds, Peroxidases in Chemistry and Biology Vol II. CRC Press, Boca Raton, FL, pp 25–50

Cooper JB, Varner JE (1983) Insolubilization of hydroxyproline-rich glycoprotein in aerated carrot root slices. Biochem Biophys Res Commun **112:** 161–167

Croft KPC, Voisey CR, Slusarenko AJ (1990) Mechanism of hypersensitive cell collapse: correlation of increased lipoxygenase activity with membrane damage in leaves of *Phaseolus vulgaris* (L.) inoculated with an avirulent race of *Pseudomonas syringae* pv. *phaseolicola*. Physiol Mol Plant Pathol **36:** 49–62

Delmer DP, Stone BA (1988) Biosynthesis of plant cell walls. *In* J Preis, eds, The Biochemistry of Plants—A Comprehensive Treatise, Vol 14: Carbohydrates. Academic Press, London, pp 373–420

Dietrich RA, Delaney TP, Uknes SJ, Ward ER, Ryals JA, Dangl JL (1994) Arabidopsis mutants simulating disease resistance response. Cell **77:** 565–577

Driouich A, Faye L, Staehelin A (1993) The plant Golgi apparatus: a factory for complex polysaccharides and glycoproteins. Trends Biochem Sci **18:** 210–214

El-Kady S, Somlyai G, Hevesi M, Klement Z (1986) Differences in antigenic structure between the wild-type and non-pathogenic mutants of *Pseudomonas syringae* pv. *phaseolicola* induced by Tn5 transposon insertions. Physiol Mol Plant Pathol **29:** 381–392

Everdeen DS, Kiefer S, Willard JJ, Muldoon EP, Dey PM, Li X-B, Lamport DTA (1988) Enzymatic cross-linkage of monomeric extensin precursors *in vitro*. Plant Physiol **87:** 616–621

Fenselau S, Balbo I, Bonas U (1992) Determinants of pathogenicity in *Xanthomonas campestris* pv. *vesicatoria* are related to proteins involved in secretion in bacterial pathogens of animals. Mol Plant Microbe Interact **5:** 390–396

Friend J (1981) Plant phenolics, lignification and plant disease. Prog Phytochem **7:** 197–261

Fry SC (1986) Cross-linking of matrix polymers in the growing cell walls of angiosperms. Annu Rev Plant Physiol **37:** 165–186

Graham MY, Graham TL (1991) Rapid accumulation of anionic peroxidases and phenolic polymers in soybean cotyledon tissues following treatment with *Phytophthora megasperma* f. sp. *glycinea* wall glucan. Plant Physiol **97:** 1445–1455

Gross GG, Janse C, Elstner EF (1977) Involvement of malate, monophenols and the superoxide radical in hydrogen peroxide formation by isolated cell walls from horseradish (*Armoracia lapathifolia* Gilib.). Planta **136:** 271–276

Hahlbrock K, Scheel D (1989) Physiology and molecular biology of phenylpropanoid metabolism. Annu Rev Plant Physiol Plant Mol Biol **40:** 347–369

Halliwell B (1978) Lignin synthesis: the generation of hydrogen peroxide and superoxide by horseradish peroxidase and its stimulation by manganese (II) and phenols. Planta **140:** 81–88

He SY, Huang HC, Collmer A (1993) *Pseudomonas syringae* pv. *syringae* Harpin Pss: a protein that is secreted via the Hrp pathway and elicits the hypersensitive response in plants. Cell **73:** 1–20

Herman EM, Lamb CJ (1992) Arabinogalactan-rich glycoproteins are localized on the cell surface and in intravacuolar multivesicular bodies. Plant Physiol **98:** 264–272

Horn MA, Heinstein PF, Low SP (1992) Characterization of parameters influencing receptor-mediated endocytosis in cultured soybean cells. Plant Physiol **98:** 673–697

Jakobek JL, Lindgren PB (1993) Generalized induction of defense responses in bean is not correlated with the induction of the hypersensitive reaction. Plant Cell **5:** 49–56

Lamb CJ, Lawton MA, Dron M, Dixon RA (1989) Signals and transduction mechanisms for activation of plant defenses against microbial attack. Cell **56:** 215–224

Leach JE, Cantrell MA, Sequeira AL (1982) Hydroxyproline-rich bacterial agglutinin from potato. Plant Physiol **70:** 1353–1358

Lindgren PB, Peet RC, Panopoulos NJ (1986) Gene cluster of *Pseudomonas syringae* pv. *phaseolicola* controls pathogenicity on bean plants and hypersensitivity on non host plants. J Bacteriol **168:** 512–522

Mäder M, Amberg-Fisher V (1982) Role of peroxidase in the lignification of tobacco cells. I. Oxidation of nicotinamide adenine dinucleotide and formation of hydrogen peroxide by cell wall peroxidases. Plant Physiol **70:** 1128–1131

Mansfield JW (1990) Recognition and response in plant-fungus interactions. *In* RSS Fraser, ed, Recognition and Response in Plant-Virus Interactions. Springer-Verlag, Berlin, pp 31–52

Mansfield JW, Brown IR, Maroofi A (1994) Bacterial pathogenicity and the plant's response: ultrastructural, biochemical and physiological perspectives. *In* DD Bills, S-d Kung, eds, Biotechnology and Plant Protection. World Scientific Publishing, Singapore, pp 85–107

Marco YJ, Rgueh F, Godiard L, Froissard D (1990) Transcriptional activation of two classes of genes during the hypersensitive reaction of tobacco leaves infiltrated with an incompatible isolate of the phytopathogenic bacterium *Pseudomonas solanacearum*. Plant Mol Biol **15:** 145–154

Martin SJ, Green DR, Cotter TG (1994) Dicing with death: dissecting the components of the apoptosis machinery. Trends Biochem Sci **19:** 26–30

Mazau D, Esquerré-Tugayé MT (1986) Hydroxproline-rich glycoprotein accumulation in the cell walls of plants infected by various pathogens. Physiol Mol Plant Pathol **29:** 147–157

Mazau D, Rumeau D, Esquerré-Tugayé MT (1988) Two different families of hydroxyproline-rich glycoproteins in melon callus. Plant Physiol **86:** 540–546

Mehdy MC (1994) Active oxygen species in plant defense against pathogens. Plant Physiol **70:** 1128–1131

Meier BM, Shaw N, Slusarenko AJ (1993) Spatial and temporal accumulation of defense gene transcripts in bean (*Phaseolus vulgaris*) leaves in relation to bacteria-induced hypersensitive cell death. Mol Plant Microbe Interact **6:** 453–466

Miller W, Mindrinos MN, Rahme LG, Frederick RD, Grimm C, Gressman R, Kyriakides X, Kokkinidis M, Panopoulos NJ (1993) *Pseudomonas syringae* pv. *phaseolicola*-plant interactions: host-pathogen signalling through cascade control of *hrp* gene expression. *In* EW Nester, DPS Verma, eds, Advances in Molecular Genetics of Plant-Microbe Interactions, Vol 2. Kluwer Academic Publishers, Dordrecht, The Netherlands, pp 267–274

Nöllenburg M, Hevesi M, Somylai G, Rudolph K, Klement Z, Kondorosi A (1990) Genetic and pathological characterization of path$^-$ and HR$^-$ mutant of *Pseudomonas syringae* pv. *phaseolicola* complemented by clones from a wild type genomic library. *In* Z Klement, ed, Plant Pathogenic Bacteria: Proceedings of the 7th International Conference on Plant Pathogenic Bacteria. Akademiai Kiado, Budapest, Hungary, pp 363–369

O'Brien TP, McCully ME (1981) The study of Plant Structure: Principles and Selected Methods. Termarcarphi, Melbourne, Australia

O'Connell RJ, Brown IR, Mansfield JW, Bailey JA, Mazau D, Rumeau D, Esquerré-Tugayé MT (1990) Immunocytochemical localization of hydroxyproline-rich glycoproteins accumulating in melon and bean at sites of resistance to bacteria and fungi. Mol Plant Microbe Interact **2:** 33–40

Peng M, Kuć J (1992) Peroxidase-generated hydrogen peroxide as a source of antifungal activity *in vitro* and on tobacco leaf discs. Phytopathology **82:** 696–699

Politis DJ, Goodman RN (1978) Localized cell wall appositions: incompatibility response of tobacco leaf cells to *Pseudomonas pisi*. Phytopathology **68:** 309–316

Pueppke SG (1984) Adsorption of bacteria to plant surfaces. *In* T Kosuge, EW Nester, eds, Plant Microbe Interactions, Molecular and Genetic Perspectives, Vol 1. Macmillan, New York, pp 215–264

Qi X, Mort AJ (1990) Co-solubilization of hydroxyproline and pectin. Is there a link between the two? (abstract No. 539) Plant Physiol **93:** S-92

Rahme LG, Mindrinos MN, Panopoulos NJ (1991) Genetic and transcriptional organization of the *hrp* cluster of *Pseudomonas syringae* pv. *phaseolicola*. J Bacteriol **173:** 575–586

Sen S (1992) Programmed cell death: concept, mechanism and control. Biol Rev **67:** 287–319

Showalter AM, Varner JE (1989) Plant hydroxyproline-rich glycoproteins. **In** A Marus, ed, Biochemistry of Plants—A Comprehensive Treatise, Vol 15: Molecular Biology. Academic Press, London, pp 485–520

Slusarenko AJ, Croft KPC, Voisey CR (1991) Biochemical and molecular events in the hypersensitive response of bean to *Pseudomonas syringae* pv. *phaseolicola*. *In* CJ Smith, ed, Biochemistry and Molecular Biology of Host-Pathogen Interactions. Clarendon Press, Oxford, UK, pp 126–143

Slusarenko AJ, Longland A, Friend J (1986) Expression of plant genes in the hypersensitive reaction of French bean (*Phaseolus vulgaris*) to the plant pathogenic bacterium *Pseudomonas syringae* pv. *phaeolicola*. *In* B Lugtenberg, ed, Recognition in Microbe-Plant Symbiotic and Pathogenic Interactions: NATO ASI Series, Vol 4. Springer-Verlag, Berlin, pp 367–376

Smith JJ, Mansfield JW (1982) Ultrastructure of interactions between pseudomonads and oat leaves. Physiol Plant Pathol **21:** 259–266

Somlyai G, Hevesi M, Bánfalvi Z, Klement Z, Kondorosi A (1986) Isolation and characterization of non-pathogenic and reduced virulence mutants of *Pseudomonas syringae* pv. *phaseolicola* induced by Tn5 transposon insertions. Physiol Mol Plant Pathol **29:** 369–380

Stakman EC (1915) Relation between *Puccinia graminis* f.sp. *tritici* and plants highly resistant to its attack. J Agric Res **4:** 195–199

Swords KMM, Staehelin LA (1993) Complementary immunolocalization patterns of cell wall hydroxyproline-rich glycoproteins studied with the use of antibodies directed against different carbohydrate epitopes. Plant Physiol **102:** 891–901

Takasugi M, Okinaka S, Katsui N, Masamune T, Shirta A, Ohuchi M (1985) Isolation and structure of lettucenin A, a novel guianolide phytoalexin from *Lactuca sativa* var. *capitata* (Compositae). J Chem Soc Chem Comm **10:** 621–622

Vance CP, Kirk T, Sherwood RT (1980) Lignification as a mechanism of disease resistance. Annu Rev Phytopathol **18:** 259–288

Vera-Estrella R, Blumwald E, Higgins VJ (1992) Effect of specific elicitors of *Cladosporium fulvum* on tomato suspension cells. Plant Physiol **99:** 1208–1215

Vianello A, Macri F (1991) Generation of superoxide anion and hydrogen peroxide at the surface of plant cells. J Bioenerg Biomembr **23:** 409–423

Whitmore FW (1978) Lignin-protein complex catalyzed by peroxidase. Plant Sci Lett **13:** 241–245

Willis DK, Rich JJ, Hrabak EM (1991) *hrp* genes of phytopathogenic bacteria. Mol Plant Microbe Interact **4:** 132–138

Woods AM, Fagg J, Mansfield JW (1988) Fungal development and irreversible membrane damage in cells of *Lactuca sativa* undergoing the hypersensitive reaction to the downy mildew fungus *Bremia lactucae*. Physiol Mol Plant Pathol **32:** 483–498